

Article

Numerical Investigation of Power Conversion Efficiency of Sustainable Perovskite Solar Cells

Vivek Bhojak ^{1,2,*}, Praveen K. Jain ¹, Deepak Bhatia ³, Shashi Kant Dargar ^{4,*} , Michał Jasinski ^{5,6,*} , Radomir Gono ^{5,6}  and Zbigniew Leonowicz ^{5,6} 

¹ Swami Keshvanand Institute of Technology, Management & Gramothan, Jaipur 302017, Rajasthan, India

² Anand International College of Engineering, Jaipur 303012, Rajasthan, India

³ Department of Electronics and Communication Engineering, Rajasthan Technical University, Kota 324010, Rajasthan, India

⁴ Kalasalingam Academy of Research and Education, Srivilliputhur 626126, Tamil Nadu, India

⁵ Department of Electrical Engineering Fundamentals, Faculty of Electrical Engineering, Wrocław University of Science and Technology, 50-370 Wrocław, Poland

⁶ Department of Electrical Power Engineering, Faculty of Electrical Engineering and Computer Science, VSB-Technical University of Ostrava, 708-00 Ostrava, Czech Republic

* Correspondence: vivek.bhojak@anandice.ac.in (V.B.); drshashikant.dargar@ieee.org (S.K.D.); michal.jasinski@pwr.edu.pl (M.J.)

Abstract: Perovskite solar cells have been researched for high efficiency only in the last few years. These cells could offer an efficiency increase of about 3% to more than 15%. However, lead-based perovskite materials are very harmful to the environment. So, it is imperative to find lead-free materials and use them in designing solar cells. This research investigates the potential for using a lead-free double-perovskite material, $\text{La}_2\text{NiMnO}_6$, as an absorbing layer in perovskite solar cells to enhance power conversion efficiency (PCE). Given the urgent need for environmentally friendly energy sources, the study addresses the problem of developing alternative materials to replace lead-based perovskite materials. Compared to single-perovskite materials, double perovskites offer several advantages, such as improved stability, higher efficiency, and broader absorption spectra. In this research work, we have simulated and analyzed a double-perovskite $\text{La}_2\text{NiMnO}_6$ as an absorbing material in a variety of electron transport layers (ETLs) and hole transport layers (HTLs) to maximize the capacity for high-efficiency power conversion (PCE). It has been observed that for a perovskite solar cells with $\text{La}_2\text{NiMnO}_6$ absorbing layer, C_{60} and Cu_2O provide good ETLs and HTLs, respectively. Therefore, the achieved power conversion efficiency (PCE) is improved. The study demonstrates that $\text{La}_2\text{NiMnO}_6$, as a lead-free double-perovskite material can serve as an effective absorbing layer in perovskite solar cells. The findings of this study contribute to the growing body of research on developing high-efficiency, eco-friendly perovskite solar cell technologies and have important implications for the advancement of renewable energy production.

Keywords: perovskite solar cell; power conversion efficiency; material optimization; LMNO



Citation: Bhojak, V.; Jain, P.K.; Bhatia, D.; Dargar, S.K.; Jasinski, M.; Gono, R.; Leonowicz, Z. Numerical Investigation of Power Conversion Efficiency of Sustainable Perovskite Solar Cells. *Electronics* **2023**, *12*, 1762. <https://doi.org/10.3390/electronics12081762>

Academic Editors: Fares M'zoughi, Izaskun Garrido, Aitor J. Garrido and Frédérique Ducroquet

Received: 6 January 2023

Revised: 15 February 2023

Accepted: 4 April 2023

Published: 7 April 2023



Copyright: © 2023 by the authors. Licensee MDPI, Basel, Switzerland. This article is an open access article distributed under the terms and conditions of the Creative Commons Attribution (CC BY) license (<https://creativecommons.org/licenses/by/4.0/>).

1. Introduction

Solar power has received a significant amount of attention from researchers in recent years because it is one of the most important renewable energy sources that have the potential to satisfy the growing energy demands on the planet. A high absorption coefficient, low excitation-binding energy, an adjustable optical bandgap, comprehensive charge carrier mobility, and low-temperature manufacturing technology are the primary requirements for an excellent solar cell [1]. Recent research has shown that perovskite materials have made significant advancements and become a crucial component in developing efficient solar cell technology [2]. The research for perovskite materials began with the investigation of calcium titanium oxide, the mineral of primary interest. The term “perovskite” refers to

any chemical substance with the same crystalline structure as calcium titanium oxide. The crystalline structure of perovskite is depicted in Figure 1. The Perovskite compounds have the chemical formula ABX_3 , where A and B both represent cations and X represents an anion that binds to both cations. According to research conducted in the past [3], the power conversion efficiency (PCE) of solar cell devices constructed from lead-based perovskite materials has the potential to reach as high as 25.2%. Perovskite solar cells are highly toxic and pose a serious health risk [4]. The challenge of lead poisoning must be overcome before commercializing these cells. In addition, device stability and efficient and cost-effective production methods are critical factors. Investigations into the effects of rain on PSC modules have raised concerns about lead and tin contamination and human health. These studies have shown that rainwater can contaminate photovoltaic solar cell modules with lead and tin.

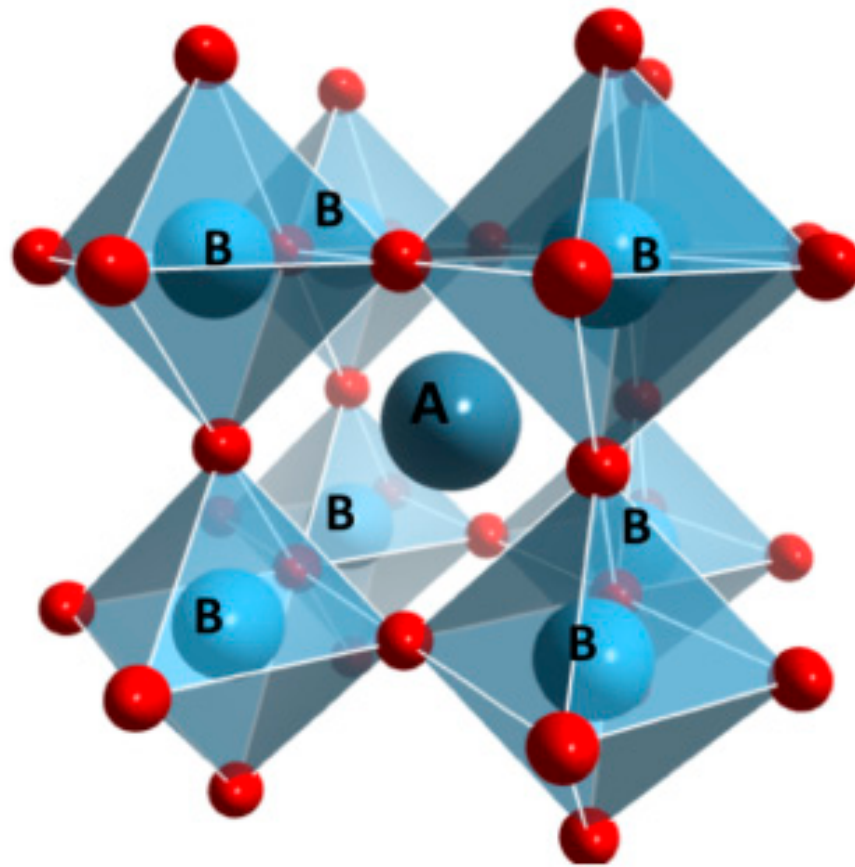


Figure 1. Structure of perovskite [5].

Long-term exposure to lead can cause anemia, paralysis, and kidney and brain damage. Even low levels of lead exposure can be fatal at high concentrations, making it a significant risk especially for pregnant women and developing fetuses. Lead can cross the placental barrier, putting the growing fetus at risk. In addition, infants exposed to lead may experience harm to their mental development. Lead exposure also increases the risk of cardiovascular disease, hypertension, and kidney disease and lowers fertility in lead-exposed individuals.

Based on the material characteristics, the solar cell developments can be categorized in three generations as depicted in Figure 2. The Perovskite solar cells have entered their third generation since their introduction, representing a type of thin-film photovoltaic technology. Depending on the context, PSCs can be developed as single-junction cells or tandem cells with multiple junctions. Perovskites possess advantageous physical, mechanical, and optoelectronic properties, making them well suited for photovoltaic (PV) applications. Researchers have combined first-principles calculation and density func-

tional theory to investigate these properties. However, the active component in traditional perovskite solar cells, which combines organic and inorganic halides, suffers from two significant drawbacks. First, the element lead (Pb) is harmful to the environment. Second, the organic cations in these materials lead to instability, shortening the shelf life of the perovskite molecule.

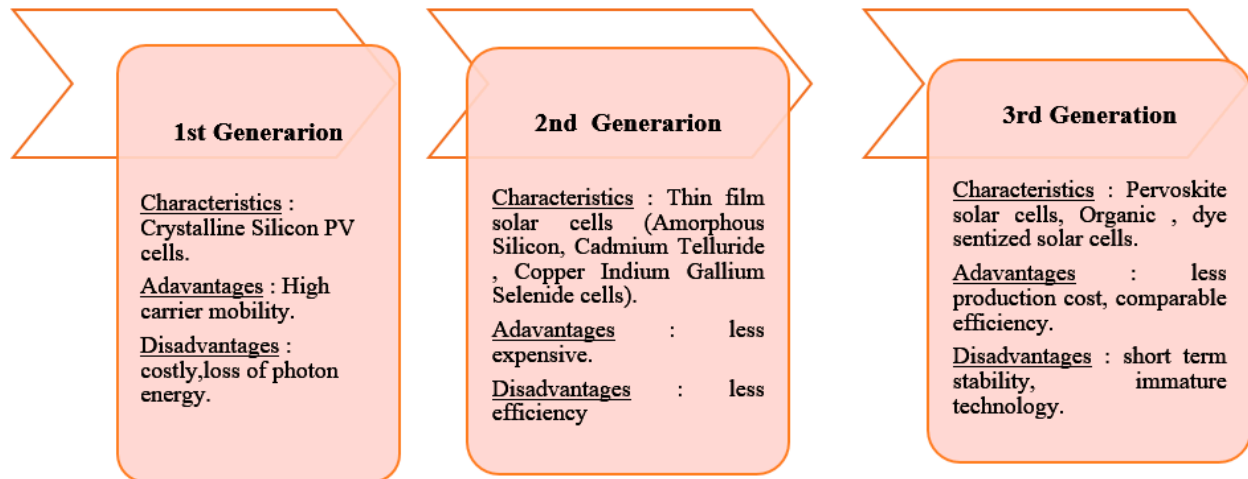


Figure 2. Generations of solar cells.

To provide the increased power conversion efficiency and various photovoltaic properties necessary for solar cell devices, lead-free materials have been the subject of a variety of theoretical and experimental studies. In order to replace lead, perovskite solar cells based on inorganic halide perovskites (such as silver, tin, bismuth, and copper) are investigated, but these devices have a bandgap greater than 2 eV, which makes them unsuitable for use in photovoltaic applications. Recent research has demonstrated that hybrid coupling can provide better performance in terms of output power and sensitivity in comparison to the linear summing of the performances of individual components. Additionally, hybridization enables the device as a whole to be adapted to various working situations, free from the limits that would otherwise be imposed by the individual functioning processes. The term “hybrid bio-nanogenerators” will henceforth refer to hybrid systems that rely on piezoelectric and triboelectric devices, are based on biocompatible materials, and are intended for the collection of clean energy from the surrounding environment and for use in biomedical applications (HBNBs). There are three types of nanogenerators—energy harvesting, wearable bioelectronics, and implantable bioelectronics—in terms of their flexibility, output voltage, output current, output power density, lifetime and reliability, ease of miniaturization, low-frequency operation, high-frequency operation, and biocompatibility [6–8]. Several research studies have examined the properties of perovskite materials, including low open-circuit voltage for Sn²⁺ cation, instability upon oxidation of Ge²⁺ cation, poor charge transport capability for bismuth, low open-circuit voltage for Sb, and weak photovoltaic qualities for Cu, among others [9]. In addition, recent research has focused on a particular class of perovskite materials known as double perovskites, which have received significant attention due to their unique properties and potential applications.

Following the universal formula ABO₃, double-perovskite structures can be produced, each of which possesses a unique combination of magnetic properties. A double-perovskite structure is produced when one B' cation replaces half of the other cations at the B site, and rock salt (NaCl) ordering is achieved. The substitution of one B for B' in the formula for A₂B₂O₆ increases the perovskite structure's original unit by a factor of 2. In addition to the flexibility and degrees of freedom offered by simple perovskite structures with one A cation site and one B cation site, a great deal of research has been done on double-perovskite compounds with two different transition metal (TM) elements at B sites (B, B') and even two different rare earth and alkaline earth elements at A sites. These compounds have

been the subject of much attention in recent years. The A site can also be occupied by two different types of cations at the A site, resulting in a perovskite with the formula $AA'BB'O_6$, referred to as both doubly ordered perovskite and double-double perovskite. Approximately 1000 different double-perovskite compounds have been synthesized, with the A site being occupied by divalent cations such as Sr, Ca, or Ba (and occasionally Pb or Cd) [10].

Double-perovskite structures offer a significant degree of flexibility in the cations that can be accommodated at the B site owing to the typical oxidation states of the B site, which are 4+ and 3+ for divalent and trivalent A cations, respectively. Practically all cations listed in the periodic table can occupy the B site of a double-perovskite structure [11]. LNMO is a ferromagnetic semiconductor composed of Ni²⁺ and Mn⁴⁺ ions, which exhibits two ferromagnetic transitions at 150 K and 280 K around its transition temperature T_c of 280 K, depending on its synthesis and heating conditions. Numerous studies have been carried out on the structural, magnetic, and optical properties of LNMO-based nanoparticles [12]. However, the greatest challenge is their practical application in devices. Recent studies have explored the medical applications of magnetic nanoparticles such as $CoFe_2O_4$, $MnFe_2O_4$, Fe_2O_3 , Fe_3O_4 , and Fe [13], but to the best of our knowledge there have been no reports on the use of double-perovskite La_2NiMnO_6 nanoparticles in medicine. La_2NiMnO_6 is a fascinating double-perovskite material with ferromagnetic properties, but its monodispersed nanoparticles are required for use in biological and medical applications due to their ability to bind and interact with biomolecules, which concentrate near the liquid–solid interface [14]. The adsorption capacity of bovine serum albumin is affected by the temperature at which the annealing process is performed. This paper employs the SCAPS-1D modelling technique to examine the absorptive properties of LNMO as an absorbing material in a heterostructure device and compares the results obtained by varying the ETLs and the work function of the front electrode. The magnetic properties of double-perovskite nanoparticles have been studied using various techniques, but their application in the biomedical field has yet to be reported. The ability of proteins to bind to surfaces has important applications in biomedical engineering, biotechnology, and environmental science.

2. Background Works

In the 1950s, a new class of materials known as double perovskites was discovered. Their usual formulas are $A_2BB'O_6$, where A represents an alkaline rare earth metal divalent ion and B and B' represent a transition, alkali, or alkaline earth metal [15]. Using various doping or composite forms makes it feasible to fine-tune the exotic features of double perovskites [16].

Moreover, aggressive light absorption, longer diffusion lengths, and low-temperature processing have proved very helpful in solar cell technology [17]. Perovskite solar cells provide a far better alternative to conventional solar cells as well as solar cells containing toxic lead for these and other reasons.

A few years ago, the efficiency of certain perovskite solar cells was just 3.8% [18], but it has since improved to as high as 22.7%. La_2NiMnO_6 , a prominent member of the double-perovskite family, is researched more often due to its unusual magneto-dielectric behaviour and near proximity to room temperature [19]. Previous work using density functional approximation reveals that the band structure of La_2NiMnO_6 allows for semiconductivity [20]. In addition, when La_2NiMnO_6 is oxidized, ferromagnetic and antiferromagnetic $LaMnO_3$ and $LaNiO_2$ are generated [21]. The amazing qualities of this material have garnered considerable attention and curiosity in recent years.

In contrast, the structure of La_2NiMnO_6 deviates somewhat from the ideal structure, with the degree of deviation varying with temperature [22]. The monoclinic phase of La_2NiMnO_6 occurs at room temperature, whereas the rhombohedral phase occurs at higher temperatures [23]. The environment and temperature effects on the characteristics and crystal structure of La_2NiMnO_6 during mixing phase have been established [24].

Double perovskites exhibit unique properties that can be fine-tuned by doping or composite forms [25]. The physical characteristics of double perovskites change when the A site is swapped due to differences in B-O-B bond angles. Calcium doping, for instance, induces a mild ferromagnetic first-order phase transition that enhances long-range ferromagnetic order. On the other hand, gadolinium doping may be utilized to improve the performance of insulating material. DFT doping has been used to improve the performance of various materials, including perovskites, carbon nanotubes, and oxides [26]. However, replicating laboratory findings via simulation can be challenging. In addition, double perovskites pose their own distinct challenges in terms of stability, performance, and efficiency when applied in various sectors. For instance, primary concerns are the pricing and potential toxicity of light-harvesting materials such as silicon solar cells and lead-halide perovskite cells. To address these limitations, extensive research has been focused on identifying suitable materials. The applicability of LMNO's monoclinic phase system in solar cells was studied by the authors of this work. Substitution doping was used to further increase light responses, and the optical examination of doped materials showed good conductivity in the visible spectrum, indicating that the system may be used in solar and energy-storage applications.

The double-perovskite material $A_2BB'O_6$, where A represents rare earth elements and B, B' represents transition metal elements, was recently found to satisfy the need for a lead-free light-absorbing layer while maintaining the typical perovskite crystal structure [27]. Due to its useful bandgap, many double-perovskite materials have been studied for application in photovoltaics [28]. These components consist of $[KNbO_3]_1 \times [BaNi_1/2Nb_1/2O_3-d]$, Bi_2CrFeO_6 , Dy_2NiMnO_6 (DNMO), Lu_2NiMnO_6 (LNMO), and La_2NiMnO_6 (LNMO). LNMO has turned to chemical processing, the simplest form of material synthesis [29] in order to produce a double-perovskite layer. By comparing the optical spectra of LNMO epitaxial films to those of $CH_3NH_3PbI_3$ with a 1.5 eV bandgap [30], Golubev et al. [31] showed the sol-gel method for polycrystalline LNMO deposition. Experiments demonstrated that LNMO crystallizes at room temperature of either a orthorhombic or a monoclinic structure and depends on the disorder or order of the sample [32]. Tai et al. [33] revealed the first experimental and theoretical analysis of the double-perovskite material LNMO and its potential usage in solar cells. They utilized both monoclinic and rhombohedral structures of LNMO together that had corresponding bandgaps of 1.4 eV and 1.2 eV, respectively. Double-perovskite LNMO with a monoclinic structure is preferred over rhombohedral structures for solar applications, according to the results [34]. Multiple investigations demonstrate that the double-perovskite LNMO possesses two ferroelectric Curie transition temperatures at temperatures of 60 K and 285 K, respectively. This material's high dielectric constant aids in the dielectric screening of photo-generated charge carriers, which is significant given that it lacks ferroelectric characteristics at ambient temperature [35]. Wang et al. [36] showed La_2NiMnO_6 for photovoltaic applications in order to further the development of lead-free inorganic double-perovskite materials, where Ln represents La, Eu, Dy, and Lu. This unique material has a longer carrier lifetime than previously known halide perovskite materials, which are comparable to silicon solar cells. The constructed device demonstrated a PCE of 0.17%, an open-circuit voltage of 336 mV, a fill factor of 0.27, and a current density of 0.27. Research on a similar double-perovskite Cs_2TiBr_6 can be found in [37,38].

The contribution of this project is the exploration and analysis of La_2NiMnO_6 as a potential absorbing material in perovskite solar cells as well as the optimization of the electron transport layers (ETLs) and hole transport layers (HTLs) to improve the power conversion efficiency (PCE) of the cells. The project also investigated the impact of varying the thickness and defect density fluctuations of the absorbing layer on PCE [39]. The motivation for this project is to develop a more efficient and cost-effective alternative to traditional silicon-based solar cells. By exploring new materials and optimizing the structure and composition of the cells, the researchers aim to improve the efficiency of solar cells and potentially lower their cost, which could contribute to the wider adop-

tion of solar energy as a clean and sustainable energy source. Additionally, the research could provide insights into the use of double perovskites, such as $\text{La}_2\text{NiMnO}_6$, in other optoelectronic applications.

3. Material and Methods

The use of numerical modelling has become more important in recent years in order to improve the understanding of physical characteristics and facilitate the construction of solar cells based on crystalline, polycrystalline, and amorphous materials. In order to achieve an advanced level of knowledge, construction, and optimization of cell structures, the use of numerical simulation is essential. It is difficult to conduct measurement analysis in the absence of a trustworthy model. The SCAPS simulator is used in this investigation to carry out a quantitative analysis of the functioning of the DPSC that is being suggested. The graphical solar cell modelling tool known as SCAPS was developed by Professor Marc Burgelman of the Electronics and Information Systems (ELIS) department at the Catholic University of Gent in Gent, Belgium. He did so by making use of National Instruments Lab Windows/CVI.

The Poisson equation, the hole continuity equation, and the electron continuity equation all contribute to the foundation of this simulation technique. Doping concentration, defect density, electron affinity, and other properties of the absorbing layer in addition to ETLs and HTLs may all influence the efficiency of power conversion. The primary objective of this research is to determine how to improve the performance of PSCs. Table 1 provides a summary of the many simulation parameters. According to previously published studies, experimental and theoretical study determines the parameters.

Table 1. Parameters of different materials.

Material Properties	TiO ₂	LMNO	C ₆₀	ZnO	Cu ₂ O	FTO	CuI
Layer thickness (nm)	30	350	30	30	200	500	200
Optical bandgap(eV)	3.2	1.05	1.7	3.3	2.17	3.5	3.1
Affinity of electron (eV)	3.9	3.52	3.9	4	3.2	4	2.1
Relative permittivity	32	3.5	4.2	9	7.11	9	6.5
Effective DOS in the conduction band (cm ⁻³)	1×10^{19}	1×10^{18}	8×10^{19}	2×10^{18}	2.2×10^{18}	2.2×10^{18}	2.2×10^{18}
Effective DOS in the valance band (cm ⁻³)	1×10^{19}	1×10^{18}	8×10^{19}	1.8×10^{19}	1.9×10^{19}	1.8×10^{19}	1.8×10^{19}
Thermal velocity of electron (cm/s)	10^7	10^7	10^7	10^7	10^7	10^7	10^7
Thermal velocity of hole (cm/s)	10^7	10^7	10^7	10^7	10^7	10^7	10^7
Mobility of electron (cm ² /Vs)	20	22	1×10^{-2}	100	3×10^2	20	100
Hole mobility (cm ² /Vs)	10	22	3.5×10^{-3}	25	8×10^1	10	47.9
Donor density (cm ⁻³)	1×10^{17}	-	2.6×10^{18}	1×10^{18}	-	1×10^{19}	-
Acceptor density (cm ⁻³)	-	7×10^{16}	-	-	1×10^{18}	-	1×10^{18}
Defect density	10^{14}	10^{14}	10^{14}	10^{14}	10^{14}	10^{14}	10^{14}

This study aims to determine how various ETLs (C₆₀, ZnO, and TiO₂) impact the device of a double-perovskite solar cell based on $\text{La}_2\text{NiMnO}_6$. The analysis has been applied to the optical absorption constant from absorption submodels sqrt (h-Eg) law (SCAPS conventional). The defect density has been set to $1 \times 10^{14} \text{ cm}^{-3}$ across all layers, while the electron and hole thermal velocities have been determined based on the structures. Interaction between 2 levels at a device's interface significantly impacts its performance.

Two interfacial flaws were considered in this device configuration, including LNMO/TiO₂ and LNMO/CuI as the displayed structures in the Figure 3.

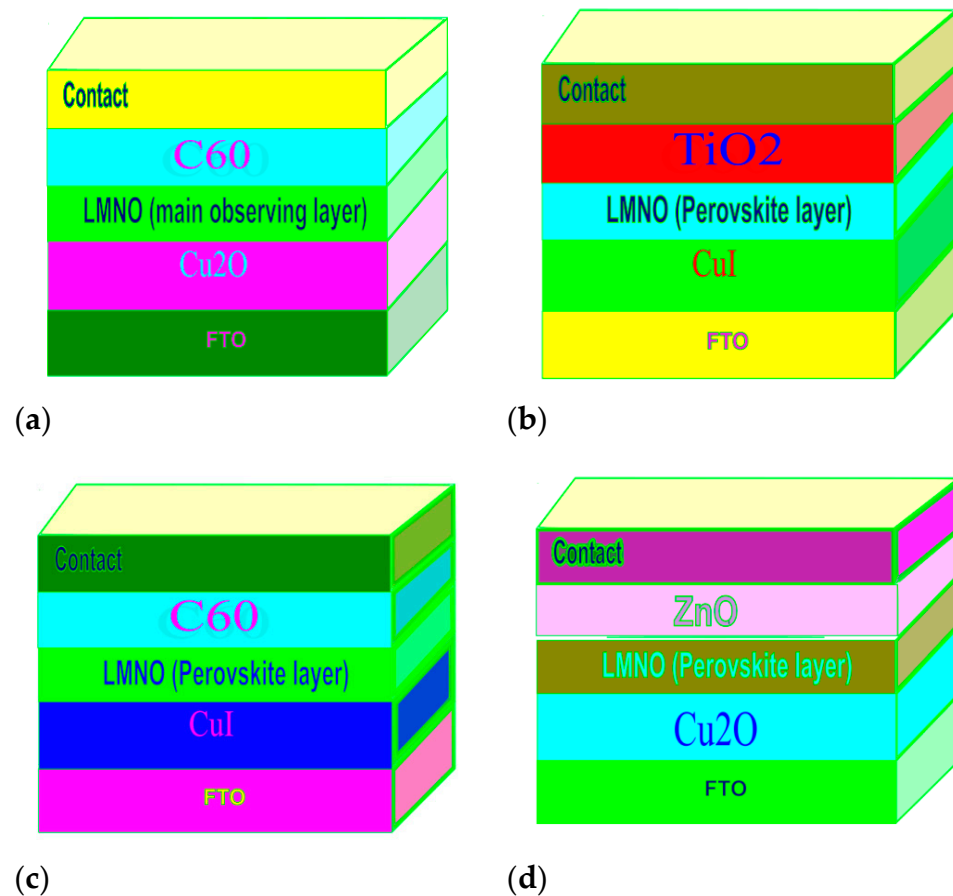


Figure 3. Schematic of various structures. (a) Structure1—C₆₀/LMNO/Cu₂O, (b) Structure2—TiO₂/LMNO/CuI, (c) Structure3—C₆₀/LMNO/CuI, (d) Structure4—ZnO/LMNO/Cu₂O.

The parameters of different materials are shown in Table 1. These parameters were used during simulation in SCAPS software.

4. Results and Discussion

This section presents the investigated characteristics of LMNO double perovskite. The bandgap is a fundamental characteristic of photovoltaic solar cell technologies. We determined that a bandgap of 1.5 eV is optimal for perovskite solar cells; thus, we adopted this value in our research. LMNO models Electron Transport Layers (ETLs) and Hole Transport Layers (HTLs) to determine the efficiency of power conversion between the two. C₆₀/LMNO/Cu₂O solar cells offer the best power conversion efficiency. This solar cell has an energy conversion efficiency of 0.43%. Cu₂O as a HTL has not been extensively studied in the past. ZnO/LMNO/Cu₂O demonstrates the lowest performance. Figure 4 shows the current densities for the different proposed structures, and it is observed that the maximum current density was observed for the C₆₀/LMNO/Cu₂O structure. Figure 5 shows the quantum efficiency of all the simulated structures, which is the function of the wavelength. It demonstrates how the quantum efficiency is varying as a function of incident wavelength in all the proposed structures. The performance parameters of simulated devices are shown in Table 2. At all interfaces and surfaces of each layer of the simulated device, the optical reflectance is set to zero.

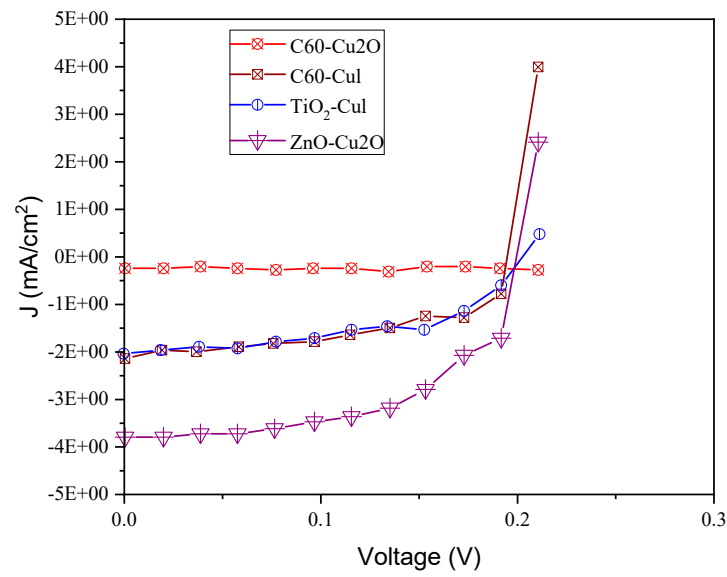


Figure 4. Current density for different structures.

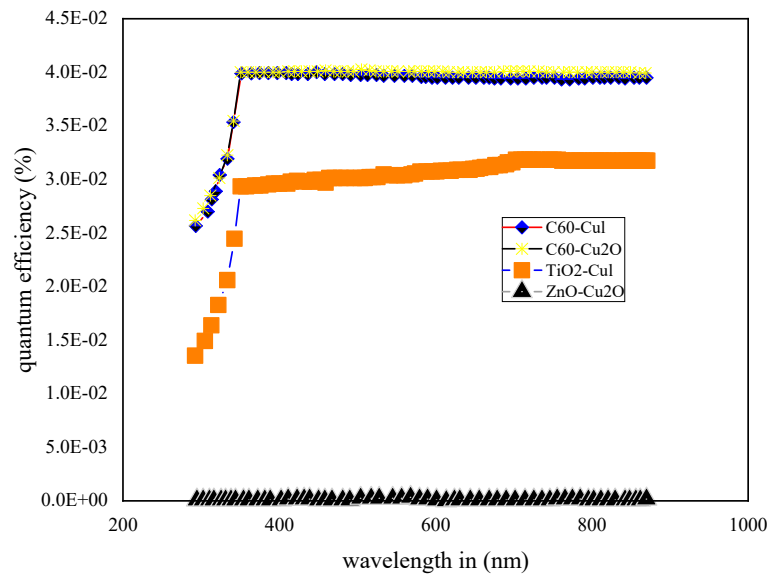


Figure 5. Quantum efficiency curve for different structures.

Table 2. Extracted results from the proposed structure.

Structure	J _{sc}	V _{oc}	FF	Efficiency (%)
C60/LMNO/Cu ₂ O	3.71	0.202	56.83	0.43
TiO ₂ /LMNO/CuI	1.92	0.1919	49.5	0.18
C60/LMNO/CuI	1.91	0.1838	48.44	0.17
ZnO/LMNO/Cu ₂ O	0.003	0.1873	52.11	0.01

4.1. Effect of Thickness

Table 3 indicates how perovskite thickness affects the efficiency and open-circuit voltage. It is essential to have a sufficiently thick absorber layer for efficient light absorption. Photon-generated electrons and holes must be able to reach the outer contact with little recombination, necessitating optimal thickness. This implies that up to a particular thickness, the power conversion efficiency increases but thereafter decreases. The greatest results are achieved using the geometry C60/LMNO/Cu₂O (efficiency 0.43). Figure 6 shows the efficiency as a function of thickness variation by adjusting the thickness of perovskite from

0.1 to 1 mm in batch simulations. It is observed that optimal performance is achieved with a thickness of 0.22 mm. As seen in Figure 7, the open-circuit voltage rises with increasing perovskite thickness.

Table 3. Effect on efficiency and Voc with thickness.

Thickness	Efficiency	Voc(V)
1.00×10^{-1}	4.20×10^{-1}	0.2009
1.00×10^0	4.30×10^{-1}	0.2018
1.50×10^0	4.30×10^{-1}	0.202
2.00×10^0	4.30×10^{-1}	0.2021

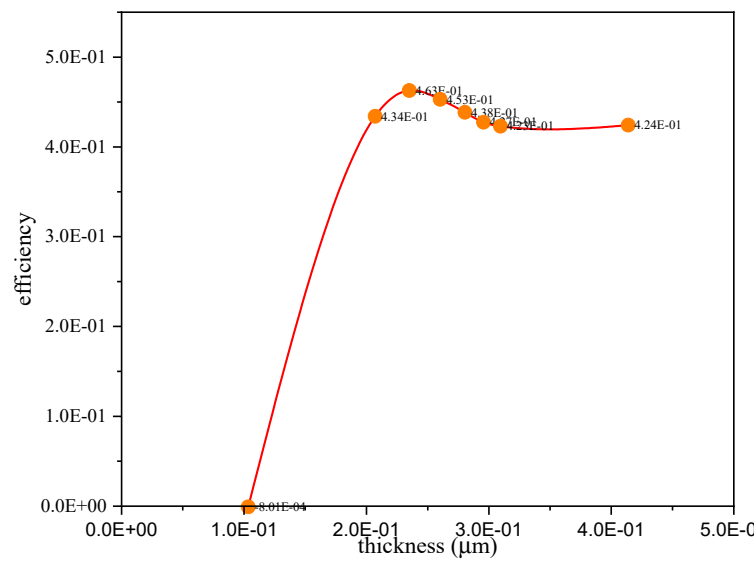


Figure 6. Schematic variation of efficiency with perovskite thickness.

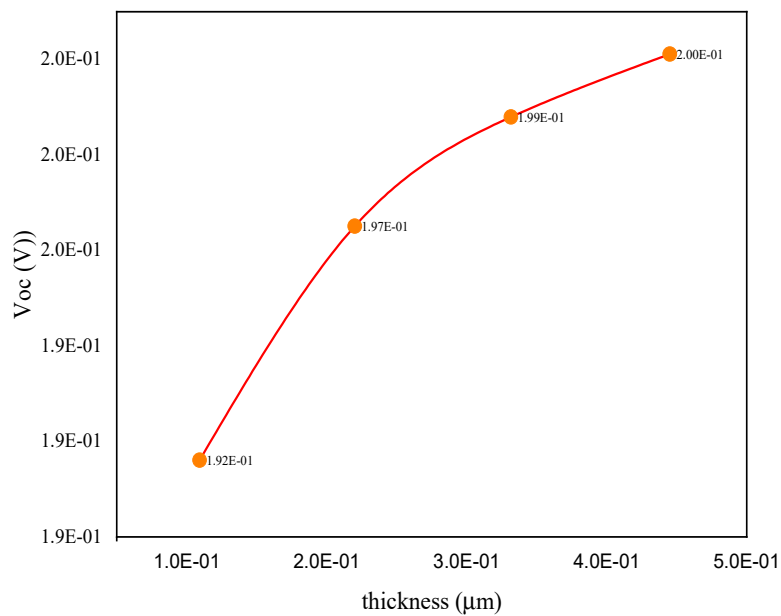


Figure 7. Variation of Voc with perovskite thickness.

4.2. Effect of Defect Density

A change in defect density occurred at $10(e) \text{ cm}^3$. It was determined that the J_{sc} saturates at a fault density of 10^9 cm^3 and that below this threshold, the parameters fluctuate

relatively minimally. Table 4 illustrates the results collected. As seen in Figures 8 and 9, defect number has a negligible impact on solar cell properties. The energy-level diagram of the corresponding structures using C60/LMNO/Cu₂O and TiO₂/LMNO/CuI is shown in Figures 10 and 11, respectively.

Table 4. Effect on efficiency and Voc with defect density.

Defect Density	Efficiency	Voc
1.00×10^{10}	4.20×10^{-1}	0.199
2.50×10^{15}	4.20×10^{-1}	0.199
5.50×10^{15}	4.20×10^{-1}	0.198
7.50×10^{15}	4.20×10^{-1}	0.198
1.00×10^{16}	4.20×10^{-1}	0.198

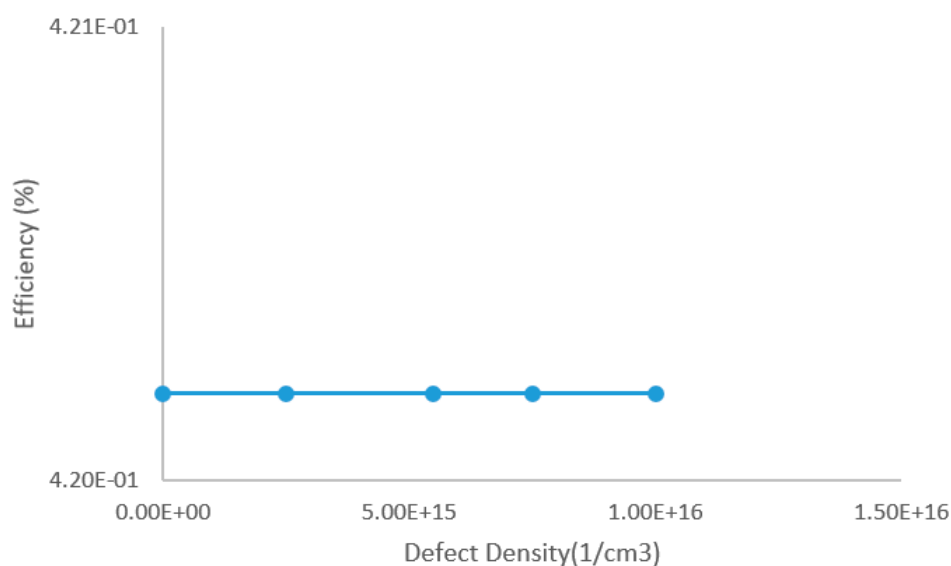


Figure 8. Variation of efficiency with defect density.

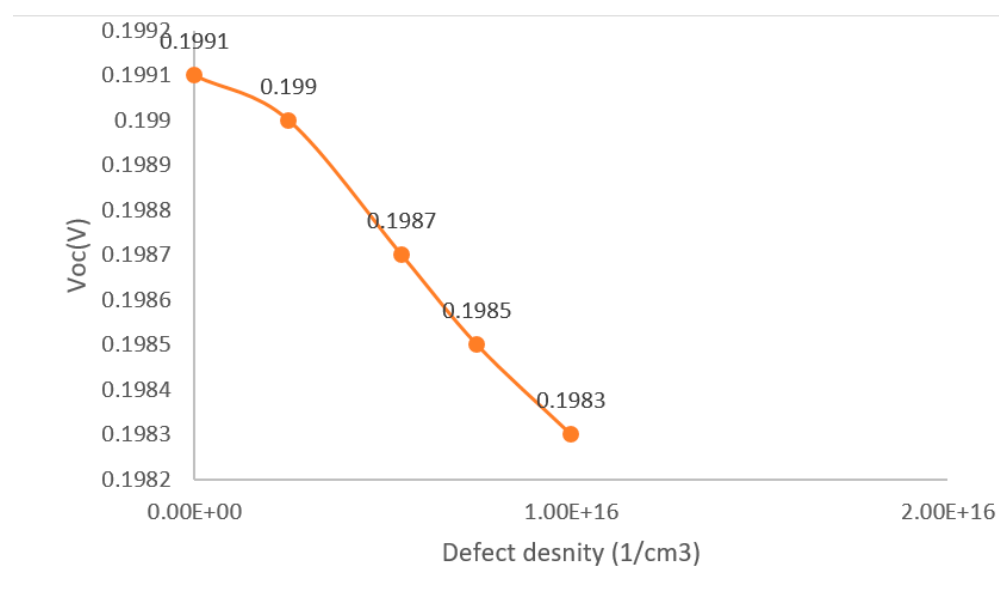


Figure 9. Variation of Voc with defect density.

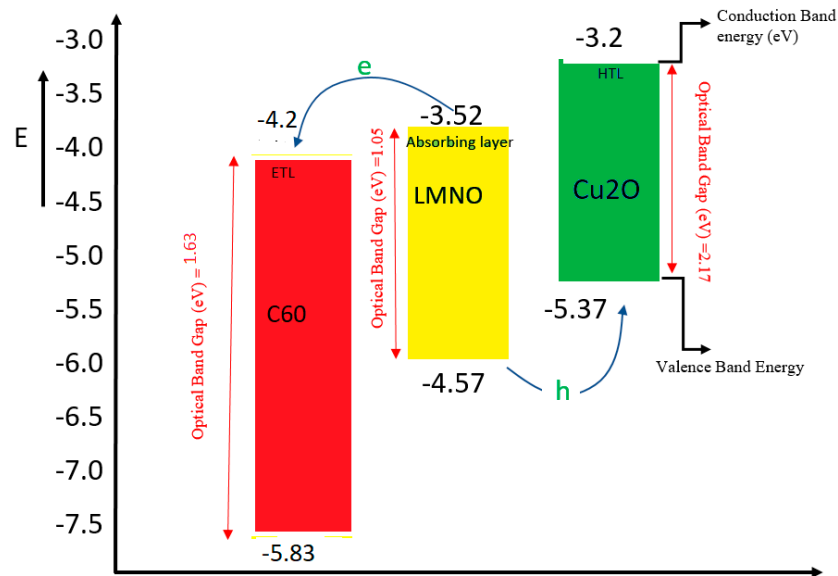


Figure 10. Energy-level diagram of structure C60/LMNO/Cu₂O.

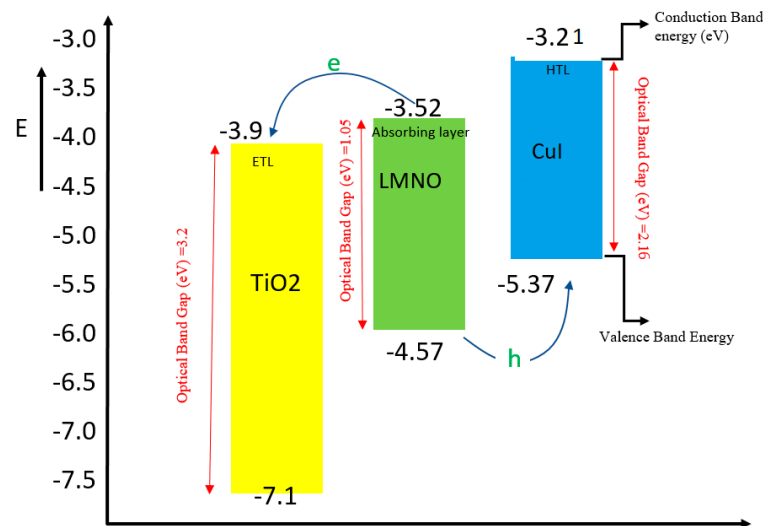


Figure 11. Energy-level diagram of structure TiO₂/LMNO/CuI.

5. Conclusions

The aim of the present study was to investigate the structural, optoelectronic, and photovoltaic properties of La₂NiMnO₆ using first principles and SCAPS-1D simulations. La₂NiMnO₆ has been shown to possess high potential as a photovoltaic material, as demonstrated by the results obtained in this work. For example, the maximum power conversion efficiency (PCE) obtained for the FTO/C60/La₂NiMnO₆/Cu₂O heterojunction in the photovoltaic investigation was 0.435%, which is significantly higher than the recently predicted value for the solar cell based on La₂NiMnO₆ (0.18%), as shown in Table 5.

Table 5. Performance comparison.

Structure	V _{OC}	J _{SC}	FF	PCE	Parameters Optimized
C60/LMNO/Cu ₂ O (Proposed)	0.1919	1.92	49.5	0.43	ETL, HTL, thickness of absorbing layer, defect density
C60/Perovskite/CuI [40]	0.1982	1.9110	47.82	0.18	ETL and work function

The thickness and defect density fluctuations of the absorbing layer were found to be the critical factors influencing PCE. However, research in $\text{La}_2\text{NiMnO}_6$ -based PSCs is still limited, and further investigation is necessary to optimize their performance. In future studies, we plan to explore the effect of doping concentration, electron affinity, different back-metal contacts, and varied hole transport layer materials of the absorber, ETLs, and HTLs on the PCE of $\text{La}_2\text{NiMnO}_6$ -based perovskite solar cells.

In summary, the present work sheds light on the high potential of $\text{La}_2\text{NiMnO}_6$ as a photovoltaic material and provides insights into the critical factors that influence its PCE. The findings of this study could help pave the way for the development of efficient and cost-effective perovskite solar cells based on $\text{La}_2\text{NiMnO}_6$.

Author Contributions: Conceptualization, V.B. and P.K.J.; data curation, V.B., P.K.J. and D.B.; formal analysis, V.B. and S.K.D.; investigation, V.B. and P.K.J.; methodology, V.B. and P.K.J.; resources, V.B. and P.K.J.; software, V.B. and P.K.J.; supervision, P.K.J. and D.B.; validation, V.B., M.J. and S.K.D.; visualization, V.B., S.K.D. and M.J.; writing—original draft, V.B., P.K.J. and D.B.; writing—review and editing, V.B., S.K.D., M.J., R.G. and Z.L.; project administrator: Z.L., founding R.G. All authors have read and agreed to the published version of the manuscript.

Funding: SGS grant was received from VSB-Technical University of Ostrava under grant number SP2023/005.

Institutional Review Board Statement: Not applicable.

Informed Consent Statement: Not applicable.

Data Availability Statement: All the data relevant to this work are available in the manuscript. Raw data and material are available on request from first author.

Acknowledgments: The authors would like to thank all the authors of the research articles used in the literature study of this work and for their reports that laid the foundation for this work.

Conflicts of Interest: The authors declare no conflict of interest.

References

1. Lee, M.M.; Teuscher, J.; Miyasaka, T.; Murakami, T.N.; Snaith, H.J. Efficient hybrid solar cells based on meso-superstructured organometal halide perovskites. *Science* **2012**, *338*, 643–647. [[CrossRef](#)]
2. Jeong, J.; Kim, M.; Seo, J.; Lu, H.; Ahlawat, P.; Mishra, A.; Yang, Y.; Hope, M.A.; Eickemeyer, F.T.; Kim, M.; et al. Pseudo-halide anion engineering for α -FAPbI₃ perovskite solar cells. *Nature* **2021**, *592*, 381–385. [[CrossRef](#)]
3. Ishikawa, R.; Watanabe, S.; Yamazaki, S.; Oya, T.; Tsuboi, N. Perovskite/graphene solar cells without a hole-transport layer. *ACS Appl. Energy Mater.* **2019**, *2*, 171–175. [[CrossRef](#)]
4. Tessler, N.; Vaynzof, Y. Preventing hysteresis in perovskite solar cells by undoped charge blocking layers. *ACS Appl. Energy Mater.* **2018**, *1*, 676–683. [[CrossRef](#)]
5. Masood, M.T.; Weinberger, C.; Sarfraz, J.; Rosqvist, E.; Sandén, S.; Sandberg, O.J.; Vivo, P.; Hashmi, G.; Lund, P.D.; Osterbacka, R.; et al. Impact of film thickness of ultrathin dip-coated compact TiO₂ layers on the performance of mesoscopic perovskite solar cells. *ACS Appl. Materials Interfaces* **2017**, *9*, 17906–17913. [[CrossRef](#)]
6. Shalenov, E.O.; Dzhumagulova, K.N.; Seitkozhanov, Y.S.; Ng, A.; Valagiannopoulos, C.; Jumabekov, A.N. Insights on desired fabrication factors from modeling sandwich and quasi-interdigitated back-contact perovskite solar cells. *ACS Appl. Energy Mater.* **2021**, *4*, 1093–1107. [[CrossRef](#)]
7. Wang, N.; Zhou, Y.; Ju, M.; Garces, H.F.; Ding, T.; Pang, S.; Zeng, X.C.; Padture, N.P.; Sun, X.W. Heterojunction-depleted lead-free perovskite solar cells with coarse-grained B- γ -CsSnI₃ thin films. *Adv. Energy Mater.* **2016**, *6*, 1670137.
8. Chung, I.; Song, J.H.; Im, J.; Androulakis, J.; Malliakas, C.D.; Li, H.; Freeman, A.J.; Kenney, J.T.; Kanatzidis, M.G. CsSnI₃: Semiconductor or metal? High electrical conductivity and strong near-infrared photoluminescence from a single material. High hole mobility and phase-transitions. *J. Am. Chem. Soc.* **2012**, *134*, 8579–8587. [[CrossRef](#)]
9. Minemoto, T.; Murata, M. Device modeling of perovskite solar cells based on structural similarity with thin film inorganic semiconductor solar cells. *J. Appl. Phys.* **2014**, *116*, 054505. [[CrossRef](#)]
10. Ma, S.; Gu, X.; Kyaw, A.K.; Wang, D.H.; Priya, S.; Ye, T. Fully Inorganic CsSnI₃-based solar cells with >6% efficiency and enhanced stability enabled by mixed electron transport layer. *ACS Appl. Mater. Interfaces* **2021**, *13*, 1345–1352. [[CrossRef](#)]
11. Wang, Y.; Tu, J.; Li, T.; Tao, C.; Deng, X.; Li, Z. Convenient preparation of CsSnI₃ quantum dots, excellent stability, and the highest performance of lead-free inorganic perovskite solar cells so far. *J. Mater. Chem. A* **2019**, *7*, 7683–7690. [[CrossRef](#)]
12. Ye, T.; Wang, X.; Wang, K.; Ma, S.; Yang, D.; Hou, Y.; Yoon, J.; Wang, K.; Priya, S. Localized electron density engineering for stabilized B- γ CsSnI₃-based perovskite solar cells with efficiencies >10%. *ACS Energy Lett.* **2021**, *6*, 1480–1489. [[CrossRef](#)]

13. Adhikari, K.R.; Gurung, S.; Bhattarai, B.K.; Soucase, B.M. Comparative study on MAPbI₃ based solar cells using different electron transporting materials. *Phys. Status Solidi C* **2016**, *13*, 13–17. [CrossRef]
14. Etgar, L.; Gao, P.; Xue, Z.S.; Peng, Q.; Chandiran, A.K.; Liu, B.; Nazeeruddin, M.K.; Grätzel, M. Mesoscopic CH₃NH₃PbI₃/TiO₂ heterojunction solar cells. *J. Am. Chem. Soc.* **2012**, *134*, 17396–17399. [CrossRef]
15. Laban, W.A.; Etgar, L. Depleted hole conductor-free lead halide iodide heterojunction solar cells. *Energy Environ. Sci.* **2013**, *6*, 3249–3253. [CrossRef]
16. Aharon, S.; Gamliel, S.; El Cohen, B.; Etgar, L. Depletion region effect of highly efficient hole conductor free CH₃NH₃PbI₃ perovskite solar cells. *Phys. Chem. Chem. Phys.* **2014**, *16*, 10512–10518. [CrossRef] [PubMed]
17. Aharon, S.; El Cohen, B.; Etgar, L. Hybrid lead halide iodide and lead halide bromide in efficient hole conductor free perovskite solar cell. *J. Phys. Chem. C* **2014**, *118*, 17160–17165. [CrossRef]
18. Xiao, L.X.; Zou, D.C. *Perovskite Solar Cells*, 2nd ed.; Peking University Press: Beijing, China, 2020.
19. Chen, J.Y.; Chen, F.X.; Xu, W.K.; Cao, G.H.; Wang, L.S. Simulation optimization of planar heterojunction perovskite solar cells with B-γ-CsSnI₃ as optical absorption layer. *J. Synth. Cryst.* **2018**, *47*, 31–36.
20. Fonash, S.J. AMPS Manual. 2010. Available online: <http://www.ampsmodeling.org/pdfs/AMPS-1D%20Manual.pdf> (accessed on 10 November 2022).
21. Lin, S.; Li, X.R.; Pan, H.Q.; Chen, H.T.; Li, X.Y.; Li, Y.; Zhou, J.R. Numerical analysis of In_xGa_{1-x}N/SnS and Al_xGa_{1-x}N/SnS heterojunction solar cells. *Energy Convers. Manag.* **2016**, *119*, 361–367. [CrossRef]
22. Ghorbani, E. On efficiency of earth-abundant chalcogenide photovoltaic materials buffered with CdS: The limiting effect of band alignment. *J. Phys. Energy* **2020**, *2*, 025002. [CrossRef]
23. Marshall, K.P.; Walton, R.I.; Hatton, R.A. Tin perovskite/fullerene planar layer photovoltaics: Improving the efficiency and stability of lead-free devices. *J. Mater. Chem. A* **2015**, *3*, 11631–11640. [CrossRef]
24. Marshall, K.P.; Walker, M.; Walton, R.I.; Hatton, R.A. Enhanced stability and efficiency in hole-transport-layer-free CsSnI₃ perovskite photovoltaics. *Nat. Energy* **2016**, *1*, 16178. [CrossRef]
25. Wu, B.; Zhou, Y.; Xing, G.; Xu, Q.; Garces, H.F.; Solanki, A.; Goh, T.W.; Padture, N.P.; Sum, T.C. Long minority-carrier diffusion length and low surface-recombination velocity in inorganic lead-free CsSnI₃ perovskite crystal for solar cells. *Adv. Funct. Mater.* **2017**, *27*, 1604818. [CrossRef]
26. Bin, Z.; Li, J.; Wang, L.; Duan, L. Efficient n-type dopants with extremely low doping ratios for high performance inverted perovskite solar cells. *Energy Environ. Sci.* **2016**, *9*, 3424–3428. [CrossRef]
27. Shao, S.; Abdu-Aguye, M.; Qiu, L.; Lai, L.H.; Liu, J.; Adjokatsé, S.; Jahani, F.; Kamminga, M.E.; ten Brink, G.H.; Palstra, T.T.M.; et al. Elimination of the light soaking effect and performance enhancement in perovskite solar cells using a fullerene derivative. *Energy Environ. Sci.* **2016**, *9*, 2444–2452. [CrossRef]
28. Konstantakou, M.; Stergiopoulos, T. A critical review on tin halide perovskite solar cells. *J. Mater. Chem. A* **2017**, *5*, 11518–11549. [CrossRef]
29. Castro, E.; Fernandez-Delgado, O.; Arslan, F.; Zavala, G.; Yang, T.; Seetharaman, S.; D'Souza, F.; Echegoyen, L. New thiophene-based C60 fullerene derivatives as efficient electron transporting materials for perovskite solar cells. *New J. Chem.* **2018**, *42*, 14551–14558. [CrossRef]
30. Shao, S.; Liu, J.; Fang, H.H.; Qiu, L.; ten Brink, G.H.; Hummelen, J.C.; Koster, L.J.A.; Loi, M.A. Efficient perovskite solar cells over a broad temperature window: The role of the charge carrier extraction. *Adv. Energy Mater.* **2017**, *7*, 1701305. [CrossRef]
31. Golubev, T.; Liu, D.; Lunt, R.; Duxbury, P. Understanding the impact of C60 at the interface of perovskite solar cells via drift-diffusion modeling. *AIP Adv.* **2019**, *9*, 035026. [CrossRef]
32. Zhao, P.; Liu, Z.; Lin, Z.; Chen, D.; Su, J.; Zhang, C.; Zhang, J.; Chang, J.; Hao, Y. Device simulation of inverted CH₃NH₃PbI₃-xCl_x perovskite solar cells based on PCBM electron transport layer and NiO hole transport layer. *Sol. Energy* **2018**, *169*, 11–18. [CrossRef]
33. Tai, Q.; Tang, K.-C.; Yan, F. Recent progress of inorganic perovskite solar cells. *Energy Environ. Sci.* **2019**, *12*, 2375–2405. [CrossRef]
34. Gao, W.; Li, P.; Chen, J.; Ran, C.; Wu, Z. Interface engineering in tin perovskite solar cells. *Adv. Mater. Interfaces* **2019**, *6*, 1901322. [CrossRef]
35. Liu, Z.; Krückemeier, L.; Krogmeier, B.; Klingebiel, B.; Márquez, J.A.; Levchenko, S.; Öz, S.; Mathur, S.; Rau, U.; Unold, T.; et al. Open-circuit voltages exceeding 1.26 V in planar methylammonium lead iodide perovskite solar cells. *ACS Energy Lett.* **2019**, *4*, 110–117. [CrossRef]
36. Wang, H.-Q.; Xu, J.; Lin, X.; Li, Y.; Kang, J.; Zheng, J.-C. Determination of the embedded electronic states at nanoscale interface via surface-sensitive photoemission spectroscopy. *Light: Sci. Appl.* **2021**, *10*, 153. [CrossRef]
37. Le Corre, V.M.; Stolterfoht, M.; Toro, L.P.; Feuerstein, M.; Wolff, C.; Gil-Escrig, L.; Bolink, H.J.; Neher, D.; Koster, L.J.A. Charge transport layers limiting the efficiency of perovskite solar cells: How to optimize conductivity. *ACS Appl. Energy Mater.* **2019**, *2*, 6280–6287. [CrossRef]
38. Bhojak, V.; Bhatia, D.; Jain, P.K. Investigation of photocurrent efficiency of Cs₂TiBr₆ double perovskite solar cell. *Mater. Today Proc.* **2022**, *66*, 3692–3697. [CrossRef]

39. Abhishek, R.; Avneesh, A.; Vinita, T. Effect of appropriate ETL on quantum efficiency of double perovskite LMNO based solar cell device via SCAPS simulation. *Mater. Today Proc.* **2021**, *47*, 1656–1659.
40. Mariello, M. Recent Advances on Hybrid Piezo-Triboelectric Bio-Nanogenerators: Materials, Architectures and Circuitry. *Nanoenergy Adv.* **2022**, *2*, 64–109. [[CrossRef](#)]

Disclaimer/Publisher’s Note: The statements, opinions and data contained in all publications are solely those of the individual author(s) and contributor(s) and not of MDPI and/or the editor(s). MDPI and/or the editor(s) disclaim responsibility for any injury to people or property resulting from any ideas, methods, instructions or products referred to in the content.